Available online at www.sciencedirect.com
SCIENCE DIRECT
Polymer 46 (2005) 9642–9652
polymer
www.elsevier.com/locate/polymer

New self-assembling biocompatible–biodegradable amphiphilic block copolymers

Francesca Signori, Federica Chiellini, Roberto Solaro*

UdR INSTM Consortium, Department of Chemistry and Industrial Chemistry, University of Pisa, Via Risorgimento 35, 56126 Pisa, Italy

Received 6 April 2005; received in revised form 23 June 2005; accepted 21 July 2005
Available online 10 August 2005

Abstract

New biodegradable–biocompatible amphiphilic block copolymers were prepared in good yields by $SnOct_2$ catalyzed ring opening polymerization of ε-caprolactone initiated by monomethoxy-terminated poly(ethylene glycol) (MPEG). Coupling of the AB copolymers with hexamethylene diisocyanate afforded ABA (formally ABBA) block copolymers. Both AB and ABA copolymers were thoroughly characterized by IR and NMR spectroscopy, size exclusion chromatography, TGA and DSC thermal analysis. In particular, DSC measurements evidenced that the copolymer hydrophilic–lipophilic balance appreciably affected the state of adsorbed water. Polarized optical microscopy of bulk materials and pyrene fluorescence emission of polymer water solutions highlighted the copolymer tendency to phase separation and self-organization, respectively. Most of the prepared materials formed micelles in water and the copolymer structure appreciably affected their critical micellar concentration. In vitro cytocompatibility tests confirmed the low toxicity of the prepared polymeric materials which enhances their potential for biomedical applications.

Keywords: Amphiphilic block copolymers; Biocompatible polymers; Self-assembly line

1. Introduction

Molecular self-assembly is a powerful approach for fabricating novel supramolecular architectures [1,2]. Usually, self-organization results from weak, non-covalent interactions (hydrogen bonds, van der Waals interaction), that guide the three dimensional organization of molecules. In the case of amphiphilic block copolymers, ordered structures are driven mainly by hydrophobic interactions [1]. As a result, when in contact with a solvent, which is selective for only one of the blocks, the material surface becomes richer in the solvent compatible block and segregation from the non-soluble block occurs. The resulting ordered structure can be dynamic (micelles) or static (nanoparticles). Many examples have been reported on amphiphilic block copolymers that give organized structures in water. These are being used as biodegradable matrices for drug delivery applications, and as self-organizing surfaces for tissue engineering [3]. Generally, the hydrophilic block is made of poly(ethylene oxide) (PEG), because of its availability, high solubility in water, and high biocompatibility. Recently, poly(*N*-vinyl-2-pyrrolidinone) was also used as hydrophilic segment, due to its high hemocompatibility [4,5]. Polystyrene [6] and poly(propylene oxide) [7] are usually chosen as the hydrophobic block.

When biodegradability is needed, the hydrophobic block is generally the degradable one, and it is usually a polyester, such as poly(lactic acid) [8], poly(lactic-*co*-glycolic acid) [9,10], poly(ε-caprolactone) [11,12]. In particular, biodegradable AB [11], ABA [13–15], and multiarm [16,17] block copolymers containing PEG and PCL segments have been developed. Amphiphilic block copolymers of malic acid and malic acid esters have also been reported to self assemble in water [18]. Micelles from amphiphilic block copolymers have recently attracted attention in various fields of medicine and biology. In particular, polymeric micelles have been developed as pharmaceutical drugs and gene delivery systems [19], as well as in diagnostic imaging

* Corresponding author. Tel.: +39 50 2219284; fax: +39 50 28438.
E-mail address: rosola@dcci.unipi.it (R. Solaro).

0032-3861/$ - see front matter © 2005 Elsevier Ltd. All rights reserved.
doi:10.1016/j.polymer.2005.07.071

techniques as carriers for various contrasting agents. For instance, ketoprofen [9], indomethacin [11], and other hydrophobic drugs [8] can be released from PEG-containing micelles. Surface functionalized micelles were obtained from functional amphiphilic block copolymers containing PEG and poly(amino acid)s [20,21].

Our group is active in the preparation and characterization of biocompatible hydrophilic polymers to be used in drug release [22–29] and tissue engineering [27–31] applications. In the present paper, we report on the synthesis and structural characterization of a series of PEG–PCL–PEG amphiphilic block copolymers containing PEG blocks of increasing length. The triblock copolymers were prepared by hexamethylene diisocyanate (HMDI) homocoupling of hydroxyl-terminated amphiphilic diblock copolymers, attained by ε-caprolactone polymerization initiated by monomethoxy poly(ethylene glycol) (MPEG). The thermal properties, behavior in bulk and in aqueous solution, self-organizing characteristics, as well as biocompatibility of both AB and ABA copolymers were also thoroughly investigated.

2. Experimental

2.1. Materials and instrumentation

2.1.1. Reagents

Toluene (Carlo Erba) was refluxed for 8 h over Na–K alloy under dry nitrogen atmosphere and then distilled, collecting the fraction having bp 110 °C. All the other solvents were dried overnight on Na_2SO_4 prior to use. ε-Caprolactone (ε-CL, Aldrich) was stirred at 60 °C on CaH_2 under dry nitrogen atmosphere and then distilled, collecting the fraction having bp 50–55 °C/0.06 mbar. Stannous (II) octoate ($SnOct_2$, Aldrich) was used as received. Hexamethylene diisocyanate (HMDI, Aldrich) was distilled under dry nitrogen atmosphere, collecting the fraction having bp 80–85 °C/0.06 mbar. Dulbecco's Modified Eagles Medium (DMEM), 0.01 M pH 7.4 phosphate buffer saline without Ca^{2+} and Mg^{2+} (PBS), fetal bovine serum (FBS), trypsine/EDTA, glutamine, and antibiotics (penicillin/streptomycin) were purchased from GIBCO Brl. Cell proliferation reagent WST-1 was purchased from Roche Diagnostic. Toluidine blue was purchased from Sigma. Cell line BALB/3T3 Clone A31 mouse embryo fibroblasts (CCL163, American Type Culture Collection) were propagated as indicated by the supplier.

2.1.2. Polymers

Monomethoxy poly(ethylene glycol)'s having molecular weight 350 (MPEG350), 750 (MPEG750), 2000 (MPEG2000), and 5000 (MPEG5000) (Aldrich) were dried by azeotropic distillation with dry toluene under dry argon atmosphere and used immediately. PCL diol (PCL2000) having $M_w = 2000$ (Aldrich) was used as received.

2.1.3. Product characterization

Thermal gravimetric analyses (TGA) were carried out under nitrogen atmosphere in the 25–700 °C range at 10 °C/min scanning rate on 10–20 mg samples by a Mettler TG 50 instrument. Onset temperatures (T_d) were evaluated as 5% weight loss. Differential scanning calorimetry (DSC) measurements were performed on 5–10 mg samples under nitrogen atmosphere by using a Mettler TA 4000 instrument. Samples were heated from 30 to 150 °C at 10 °C/min (1st heating), cooled to −150 °C at the same scan rate (1st cooling), then heated again to 150 at 10 °C/min (2nd heating). Samples were then quenched to −150 °C at −100 °C/min, kept at this temperature for 2 min, and finally heated again to 150 °C at 10 °C/min (3rd heating). Glass transition temperatures were measured from the inflection point in the third heating thermogram; melting enthalpies were evaluated from the integrated areas of melting peaks by using indium for calibration. Melting point determinations and microscopy observations were performed by a Reichert–Jung Polyvar microscope equipped with Mettler FP52 hot plate.

FT-IR spectra were recorded under dry nitrogen atmosphere on liquid films, cast polymer films, and KBr pellets with a Jasco 4100 FT-IR spectrophotometer. ^1H NMR spectra were recorded at 200 MHz on 5–10% sample solutions in perdeuterated solvents with a Varian Gemini 200 spectrometer, by using the following experimental conditions: 11,968 data points, 3 kHz spectral width, 30° pulse, 2 s acquisition time, 1 transient. Peak multiplicity was denoted as by following: s, singlet; d, doublet; dd, double doublet; t, triplet; q, quartet; m, multiplet; brs, broad signal. Size exclusion chromatography (SEC) analyses were performed in $CHCl_3$ at 20 °C, by using a HPLC Water 510 pump equipped with two Mixed-D PLgel columns (300×7.5 mm), a PLgel guard column (50×7.5 mm), and a Water 410 refraction index detector. Monodispersed poly(ethylene glycol) samples (Fluka) were used as calibration standards. Optical microscopy analyses were performed by a Reichert–Jung Polivar microscope, equipped with Mettler FP52 hot plate and Mettler FP5 temperature controller. Polymer films were cast on glass slides from 1% chloroform solution, evaporated in dry atmosphere for 24 h, and finally dried 12 h under vacuum. The films were heated at 85 °C, left at this temperature for15–20 min in order to remove residual moisture traces, and then cooled down to 30 °C at either 2 or 100 °C/min. Samples for fluorescence measurements were prepared from 1 g/l polymer solution and 0.12 mg/l (0.6 μM) pyrene stock solutions in Millipore water. Pyrene concentration in each sample was 3×10^{-7} M, whereas polymer concentrations ranged between 500 and 0.02 mg/l. Fluorescence spectra were recorded at 25 °C by using a Perkin–Elmer LS 55 spectrofluorimeter, using 2.5 nm slit openings. Fluorescence

excitation (λ_{em} 390 nm) spectra were recorded in the 300–360 nm range, respectively.

2.1.4. Biological tests

Cell adhesion and proliferation assays were carried out using the 3T3/BALB-C Clone A31. Cell were grown in DMEM containing 10% FBS, 4 mM glutamine, and 100 U/ml:100 μg/ml penicillin:streptomycin (complete DMEM).

2.1.4.1. Subculturing. A 25 ml flask containing exponentially growing 3T3 cells was observed under an inverted microscope for cell confluence. The complete DMEM media was then removed and cells were rinsed for few minutes with PBS. The buffer solution was removed and cells were incubated with 0.5 ml of trypsin/EDTA solution at 37 °C in 5% CO_2 incubator for 5 min or until the monolayer started to detach from the flask. Cells were suspended in 5 ml of complete DMEM media and then centrifuged at 700*g* for 5 min. The pellet was suspended in an appropriate volume of DMEM and plated at a split ratio of 1:6 or 1:10 in a 75 ml flask.

2.1.4.2. Direct contact assays. Polymer films were prepared by slow solvent evaporation of 1% chloroform solution of the polymer cast on glass slides. The polymer films were carefully dried under vacuum, incubated in PBS, and then UV sterilized for 10–15 min. Cells were seeded at appropriate density; the polymer film was placed in direct contact with cell monolayer and cell adhesion was checked 2 h later. The culture medium was then removed, thus removing also the cells that did not adhere, and replaced with fresh complete DMEM. Cells were allowed to proliferate for 72 h and then evaluation of cell viability was carried out by mean of WST-1 assay as well as by morphological investigation on fixed and stained cells.

2.1.4.3. Determination of IC_{50} of soluble polymers. The IC_{50} (50% inhibitory concentration, that is the material concentration at which 50% of cell death in respect to the control is observed) of soluble polymeric materials was evaluated by exposing cells for 24 h to DMEM containing different polymer concentrations. At the end of the exposure time, cells were incubated with WST-1 cell proliferation reagent for the quantitative evaluation of cell proliferation.

2.1.4.4. Cell proliferation assay. Quantitative proliferation was assayed by using the cell proliferation reagent WST-1 and by following the protocol indicated by the manufacturer. Briefly, cells were allowed to proliferate either in direct contact with polymeric materials or exposed to DMEM containing different concentration of polymer and then incubated for 4 h with an appropriate volume of WST-1 tetrazolium salts. Formazan production was detected at 450 nm, with 620 nm as reference wavelength using an ELISA microplate reader (Biorad.).

2.1.4.5. Cell fixing and staining. Cells grown in contact with polymeric materials were washed three times with PBS, incubated for 1 h at room temperature in a 3.8% solution of paraformaldehyde in 0.01 M pH 7.4 PBS, and finally carefully rinsed with PBS. For post-fixation staining, cells were incubated with toluidine blue solution in PBS, rinsed with PBS, and stored at 4 °C.

2.1.4.6. Microscopy. For routine culturing and qualitative evaluation of morphology, cells were analyzed under an inverted microscope Nikon Eclipse TE2000-U.

2.2. Polymer synthesis

Polymerizations experiments were carried out according to general procedures. Data relevant to each run are summarized in Tables 1 and 2, whereas two typical procedures are reported in the following.

2.2.1. Preparation of MPEG350-PCL copolymer (Run PC1)

A solution of 5.0 g (14.3 mmol) of MPEG350 in 20 ml toluene was refluxed for 3 h under dry nitrogen atmosphere. After distilling off the toluene–water azeotrope, excess toluene was removed under vacuum. Anhydrous ε-caprolactone (16.3 g, 0.143 mol) and $SnOct_2$ (0.21 g, 0.52 mmol) were added, and the polymerization mixture was stirred for 24 h at 120 °C. The crude product was dissolved in acetone, and coagulated in diethyl ether at 0 °C, to give 14.4 g (68% yield) of a white powder.

FT-IR (cast film): 3438 (νOH), 2945 (νCH_3), 1725 (νC=O), 1107 cm^{-1} (νC–O). ^{1}H NMR (200 MHz, $CDCl_3$, ppm) δ: 4.2 (t, OCH_2CH_2OCO), 4.0 (t, CH_2OCO), 3.6 (brs, OCH_2CH_2O), 3.3 (s, CH_3O), 2.3 (t, CH_2COO), 1.6 (m, CH_2), 1.4 (m, CH_2).

2.2.2. Preparation of MPEG350-PCL-MPEG350 copolymer (Run C1)

About 20 ml of toluene–water azeotrope was distilled off a solution of 10 g (5.5 mmol) of PC1 in 50 ml toluene. After cooling at room temperature, a solution of 0.46 g (2.7 mmol) of HMDI in 5 ml of dry toluene was added. The reaction mixture was kept under stirring at 80 °C for 18 h, while monitoring the disappearance of the 2265 cm^{-1} absorption band by FT-IR analysis. The crude reaction product was coagulated into anhydrous *n*-heptane to give 9.9 g (95% yield) of polymeric product.

FT-IR (cast film): 3437 (νOH), 3391 (νNH), 1725 (νC=O ester), 1628 cm^{-1} (νC=O carbamate). ^{1}H NMR (200 MHz, $CDCl_3$, ppm) δ = 4.8 (brs, NH), 4.2 (t, OCH_2CH_2OCO), 4.0 (t, CH_2OCO), 3.6 (brs, OCH_2CH_2O), 3.3 (s, CH_3O), 3.2 (m, $NHCH_2$), 2.3 (t, CH_2COO), 1.7–1.3 (m, CH_2).

Table 1
Preparation of AB amphiphilic block copolymers

Run[a]	MPEG		$SnOct_2$ (mmol)	Yield (%)	PCL block[b] (DP_n)	Copolymer M_n		M_w/M_n[c]
	(MW)	(mmol)				Calculated[d]	By SEC[c]	
PC1	350	14.3	0.52	68	11	1600	1900	1.4
PC2	750	6.7	0.32	94	10	1890	2050	1.3
PC3	2000	5.0	0.39	91	10	3140	3200	1.2
PC3b[e]	2000	10.0	0.78	92	4.5	2500	2450	1.1
PC4	5000	5.0	0.76	92	10	6140	5500	1.1

[a] In 20 ml toluene at 120 °C for 24 h; ε-CL/MPEG molar ratio = 10.
[b] By ^{1}H NMR.
[c] PEG standards.
[d] From the feed composition.
[e] ε-CL/MPEG molar ratio = 5.

3. Results and discussion

3.1. Synthesis and structural characterization of block copolymers

Linear AB copolymers were easily prepared by addition of ε-caprolactone (ε-CL) to monomethoxy poly(ethylene glycol) (MPEG) in the presence of stannous octoate ($SnOct_2$) as catalyst (Scheme 1). The choice of the catalyst was suggested by its high efficacy in promoting ring opening polymerization of ε-CL, and because of its low toxicity, which resulted in FDA (Food and Drug Administration) approval for biomedical uses.

Polymerization experiments were carried out in bulk at 120 °C for 24 h (Table 1), then the crude products were dissolved in acetone and coagulated into cold (0 °C) diethyl ether. Yields larger than 90% were attained in most cases. The use of MPEG samples having molecular weight included between 350 and 5000 allowed for attaining copolymers with different hydrophilic–lipophilic balance. The ε-CL/MPEG molar ratio was generally kept constant at 10, to obtain PCL segments of comparable length. In order to investigate the influence of the PCL block length, sample PC3b was prepared starting from MPEG2000 and by using 5:1 ε-CL/MPEG molar ratio. The copolymer chemical compositions were evaluated from the relative intensities of ^{1}H NMR signals at 2.3 and at 3.7 ppm, attributed to one methylene group of PCL repeating units and to all MPEG methylene groups, respectively. The degree of polymerization of the PCL block was evaluated from the relative intensity of peaks at 4.0 and 4.2 ppm, attributed to the esterified methylene group belonging to PCL repeating units and terminal methylene of MPEG block, respectively.

In all cases the degree of polymerization (DP_n) evaluated by NMR was quite close to that computed from the feed composition. Furthermore, comparison of the intensity of the signal at 3.3 ppm, attributed to MPEG methoxy group with that of the peak at 4.2 ppm confirmed that all MPEG molecules were actually bound to PCL segments. In agreement, low molecular weight peaks attributable to either unreacted MPEG or short PCL chains were absent from the SEC chromatograms of the copolymerization products. In all cases, SEC analysis showed monomodal, relatively narrow molecular weight distributions. Additionally, the molecular weights evaluated from the NMR PEG/PCL ratio and by SEC were in satisfactory agreement (Table 1). All copolymer samples were insoluble in diethyl ether at 0 °C, where low molecular weight MPEG samples are soluble. This behavior is again in accordance with the formation of MPEG–PCL copolymer molecules. Independently of the PEG segment length, all AB copolymers were soluble in polar organic solvents, such as chloroform,

Table 2
Preparation of ABA amphiphilic block copolymers

Run	PC*x*		Time (h)	Yield (%)	Copolymer M_n		M_w/M_n[a]	PC*x*[b] (%)	Solubility[c] (g/l)
	M_n[a]	(mmol)			Calc.[d]	By SEC[a]			
C1	1900	5.5	18	95	4000	4250	1.3	4	3
C2	2050	4.7	20	91	4300	3700	1.5	19	8
C3	3200	1.5	24	94	6600	5200	1.3	20	12
C3b	2450	4.0	24	99	5100	5050	1.1	0	24
C4	5500	2.0	24	96	11,200	10,000	1.3	20	>40

In 35 ml of anhydrous toluene at 80 °C; PC*x*/HMDI = 2.
[a] PEG standards.
[b] Unreacted PC*x*.
[c] In water at 25 °C.
[d] Calculated from the feed composition.

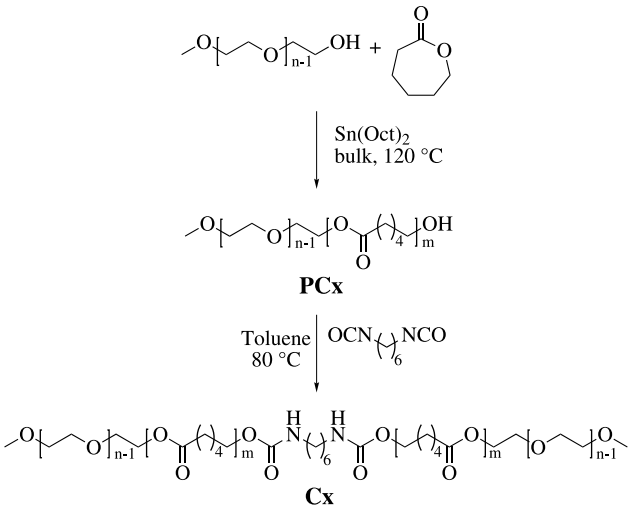

Scheme 1. Preparation of AB and ABA amphiphilic block copolymers.

acetone, and dimethylsulfoxide. On the other hand, a water solubility appreciably larger than1.0 g/l was shown only by samples PC3 (6 g/l), PC3b (21 g/l) and PC4 (20 g/l) having favorable hydrophilic/hydrophobic balance.

The prepared AB MPEG–PCL copolymers were used as building blocks for the preparation of ABA (formally ABBA) amphiphilic block copolymers (Scheme 1), containing a central, hydrophobic PCL chain linked to two identical MPEG lateral segments. Hexamethylene diisocyanate (HMDI) was selected as coupling agent because of low cost, high reactivity with primary hydroxyl groups, and low toxicity of the biodegradation products of its urethane derivatives [32]. A 2:1 PC*x*/HDMI molar ratio was used in all cases. Coupling reactions were carried out in dry toluene at 80 °C, to avoid HMDI thermal degradation. The reaction was monitored by FT-IR analysis, until complete disappearance of the isocyanate IR absorption band at 2265 cm^{-1}. Reaction times of 18–24 h were used in all cases, longer reaction times being necessary for samples containing higher molecular weight PEG chains. Crude products were purified by coagulation in cold (0 °C) anhydrous *n*-heptane, where HMDI is soluble. As expected, FT-IR spectra of all samples presented the diagnostic band of carbamate bonds at 1620–1630 cm^{-1}. Copolymer compositions were determined by ^1H NMR analysis. Due to the structural symmetry of ABA copolymers, their PEG/PCL ratio resulted identical to that of the corresponding AB precursors. The effective copolymer structure was evaluated from the relative intensity of the signal at 3.2 ppm, attributed to methylene groups bound to the carbamate nitrogen. However, partial overlapping of diagnostic peaks somewhat limited the accuracy of NMR structural characterization.

The copolymer molecular weights, as evaluated by SEC analysis closely corresponded to those computed from the feed composition (Table 2). However, most SEC peaks presented a low molecular weight shoulder having the same molecular mass as the corresponding PC*x* precursors. The amount of unreacted PC*x* (Table 2) was evaluated by deconvolution of the molecular weight distribution curves (Fig. 1).

This finding can be attributed to the reaction of HMDI with moisture traces still present in PC*x* macromonomers. It is also possible that PC*x* hydroxyl end groups undergo thermal degradation during anhydrification by azeotropic distillation. Indeed, PC*x* solutions turned yellowish during this treatment. Purified C2 (M_n = 4200, M_w/M_n = 1.2), C3 (M_n = 6500, M_w/M_n = 1.1), and C4 (M_n = 12,500, M_w/M_n = 1.1) samples containing less than 3% of PC*x* macromonomers were obtained in 30–40% yield by repeated fractional precipitation from dichloromethane into cold *n*-heptane. All measurements were performed on these purified samples.

The solubility behavior of ABA polymers in polar aprotic solvents was similar to that of the corresponding AB building blocks, indicating that the presence of two carbamate bonds and doubling of the molecular weight did not appreciably affect material solubility characteristics. However, all ABA copolymer resulted soluble in water and their water solubility significantly increased on increasing the length of the PEG segment. The very large difference between the water solubility of AB and ABA copolymers demonstrates that the distribution of hydrophilic and hydrophobic blocks indeed affected the copolymer solubility behavior.

3.2. Thermal analysis

The polymer thermal stability was evaluated by TGA analysis under nitrogen atmosphere. All analyzed samples presented less than 4% mass residue (WR_{700}) at 700 °C. The onset decomposition temperature (T_d) of MPEG samples, evaluated as 5% weight loss, increased from 192 to 355 °C on increasing the PEG degree of polymerization from about 7 to 113 (Table 3). The T_d of PCL diol having 2000 average

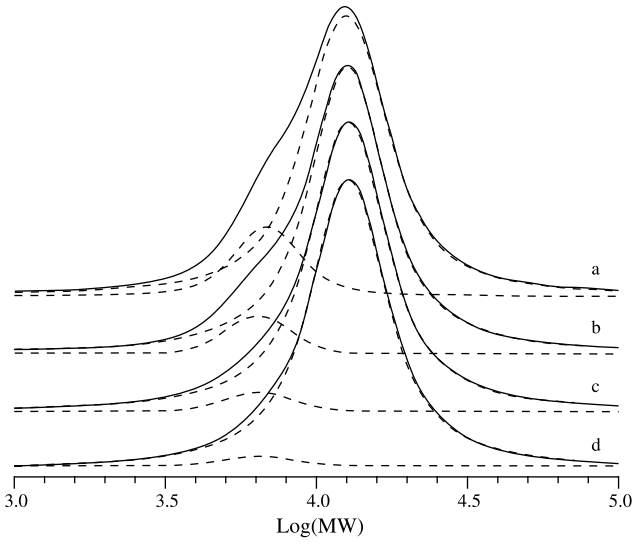

Fig. 1. Deconvolution of the molecular weight distribution of sample C4: Unfractionated (a), after 1 (b), 2 (c), and 3 (d) fractional precipitations in *n*-heptane.

molecular weight (PCL2000), a suitable model of the PCL block in ABA copolymers, was comparable to that of MPEG2000. In all cases, the decomposition onset of AB and ABA polymers occurred in the 280–310 °C range. No simple dependence of copolymer T_d on PEG chain length was observed. PCL2000 and all MPEG samples displayed a single decomposition process. On the other hand, all PC*x* and C*x* copolymers displayed two partially overlapping steps. The inflection temperature of the first decomposition stage (T_{d1}) was in the 320–360 °C interval for AB samples and between 310 and 360 °C for ABA polymers. The inflection temperature of the second decomposition step (T_{d2}) ranged from 390 to 410 °C and from 390 to 440 °C for AB and ABA copolymers, respectively. Moreover, the inflection temperature of both steps decreased on increasing the PEG block length. It is worth noting that the relative extent of the first decomposition process (Δw_1) strongly decreased on increasing the PEG/PCL ratio. This behavior suggests that the decomposition of PCL segments was responsible for the lower temperature step, whereas PEG domains degraded at higher temperature.

The thermal behavior of the investigated polymeric materials was examined by DSC analysis (Table 4). As expected, the crystallization (T_c) and melting (T_m) temperatures as well the corresponding crystallization (ΔH_c) and melting (ΔH_m) enthalpies of MPEG samples steadily increased on increasing the PEG chain length. It is worth noting that MPEG350 and MPEG750 presented composite endothermic peaks. This behavior was attributed to the melting of PEG lamellae with different fold numbers [33].

The low glass transition temperature (T_g) of low molecular weight MPEG's confirmed the rather high flexibility of PEG chains. On the other hand, no glass transition was detected for MPEG2000 and MPEG5000, possibly because of extensive crystallization. PCL2000, the model of PCL blocks, presented a T_g of −58 °C, and a bimodal melting pattern with maxima at 58 and 64 °C. AB and ABA block copolymers showed only one glass transition. Their T_g was included between −58 and −51 °C and between −55 and −48 °C, respectively. Only the T_g of C3b sample was somewhat higher (−34 °C). This finding indicates that copolymer macromolecules have comparable mobility. Although phase separated block copolymers are expected to display two distinct glass transitions, the presence of just one glass transition can be attributed to the very similar T_g of MPEG and PCL segments.

On heating, the DSC traces of copolymers showed one ill-resolved, complex endothermic peak (Figs. 2 and 3). Only PC1, PC2, C1, and C2, containing short PEG blocks showed distinct overlapping peaks. A similar behavior was observed on cooling. PC1 and C1 samples presented melting and crystallization temperatures and enthalpies close to those of PCL, very likely because of their large PCL/PEG ratio [13]. On increasing the molecular weight of the PEG block, both transition temperatures and enthalpies shifted towards the values typical of the corresponding MPEG components. Apparently, PEG and PCL blocks crystallized separately, although the presence of two different phases perturbed the crystallization process.

3.3. Polarized optical microscopy

The optical micrographs of representative AB and ABA block copolymers observed under crossed polarizers are reported in Fig. 4. Spherulites constituted by alternating bright and dark bands were present in PC1 and C1 in which the molecular weight of PEG blocks is appreciably lower than that of the PCL segment. Similar extinction rings were observed for PCL in polymer blends [34,35] and in AB block copolymers containing PEG and PCL segments of comparable molecular weight [36]. Depending on the crystallization conditions, MPEG5000 containing copolymers (PC4 and C4) displayed either single-circle spherulites

Table 3
Thermal gravimetric analysis (TGA) of the investigated polymeric materials

Sample	MPEG (%wt)	T_d (°C)	T_{d1} (°C)	Δw_1 (%wt)	T_{d2} (°C)	Δw_2 (%wt)	WR_{700} (%wt)
MPEG350	100	192	332	99.9	–	–	0.1
MPEG750	100	273	409	99.6	–	–	0.4
MPEG2000	100	331	408	99.7	–	–	0.3
MPEG5000	100	355	389	99.9	–	–	0.1
PCL2000	0	338	424	99.9	–	–	0.1
PC1	22	294	362	95.0	410	4.0	1.0
PC2	40	281	360	67.5	410	32.2	0.3
PC3	64	306	355	37.2	414	59.8	3.0
PC3b	80	291	321	21.0	392	78.3	0.7
PC4	81	302	339	17.9	391	81.1	1.0
C1	22	301	357	94.0	436	5.7	1.3
C2	40	295	345	68.7	403	28.0	3.3
C3	64	301	340	36.2	419	63.4	0.4
C3b	80	292	314	20.2	394	77.2	2.6
C4	81	293	316	17.5	388	82.4	0.1

T_d is the onset decomposition temperature, evaluated as 5% weight loss; T_{d1} and T_{d2} are the temperatures at the inflection point of the first and second decomposition steps; Δw_1 and Δw_2 are the weight losses of the first and second decomposition steps; WR_{700} is the mass residue at 700 °C.

Table 4
DSC analysis of the investigated polymeric materials

Sample	T_g[a] (°C)	ΔC_p (J/g K)	T_c[b] (°C)	ΔH_c[c] (J/g)	T_m[d] (°C)	ΔH_m[c] (J/g)
MPEG350	−79	0.21	−36, −22	−93	−12, 7	107
MPEG750	−59	0.20	10	−118	30 (s), 42	121
MPEG2000	nd	nd	30	−170	69	174
MPEG5000	nd	nd	37	−178	75	185
PCL2000	−52	0.20	20	−65	58, 64	67
PC1	−58	0.26	25	−78	55, 60	79
PC2	−54	0.25	−5, −1, 14	−88	33 (s), 41, 49	83
PC3	−54	0.15	26	−116	64	128
PC3b	−55	0.25	27	−122	63	126
PC4	−51	0.16	34	−134	72	140
C1	−54	0.20	21	−62	55, 60	65
C2	−55	0.31	−33, −3, 18	−73	6, 26, 44, 49	78
C3	−48	0.17	22	−104	63	109
C3b	−34	0.15	17	−110	63	113
C4	−50	0.10	39	123	64	135

[a] Evaluated from the third heating cycle after quenching at −100 °C/min; nd = not detected.
[b] Evaluated from the first cooling cycle.
[c] In the case of multiple peaks, ΔH is the overall enthalpy.
[d] Evaluated from the second heating cycle; s = shoulder.

or concentric spherulitic structures. Copolymers based on MPEG750 and MPEG2000 presented an intermediate crystallization behavior. On the other hand, the C3b sample, having the lowest PCL/PEG ratio formed only very large PEG spherulites, very likely because of the low tendency of the short PCL segments to crystallize. By taking into account the sample chemical composition, the inner and the outer spherulites were attributed to PCL and PEG components, respectively, whereas the large single-circle spherulites must be assigned exclusively to PEG segments. The faster nucleation of PCL in PEG/PCL blends and the higher crystallization rate of PEG with respect to PCL segments [36] are in agreement with the observed crystallization behavior and support the proposed attributions.

3.4. State of water

Water in hydrophilic polymers can exist in a number of different states ranging from normal bulk-like water to water molecules hydrogen-bonded to hydrophilic groups of the polymer chain. This behavior is usually approximated by a three-state model [37], which hypothesizes the existence of three different states of water, that is: free water, bound water and interfacial water. Free water is constituted by molecules not bound to the polymer and it is characterized by melting temperature and enthalpy similar to those of pure water [38,39]. Interfacial water weakly interacts with the polymer and is characterized by a phase transition temperature significantly lower than 0 °C. The bound water strongly interacts with polymer chains and no detectable phase transition is observed in the 200–273 K temperature range, usually associated with water freezing/melting transitions [38,40]. According to some authors, bound water is trapped within polymer microcavities. This water cannot freeze because there are not enough water molecules to form a crystal and in any case the nucleation rate is too small [41].

The state of adsorbed water in the hydrated polymeric systems was investigated by DSC analysis of block

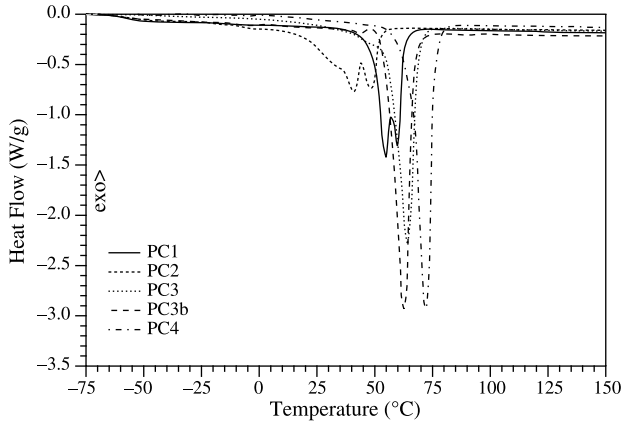

Fig. 2. DSC heating curves (10 °C/min) of PC*x* copolymers.

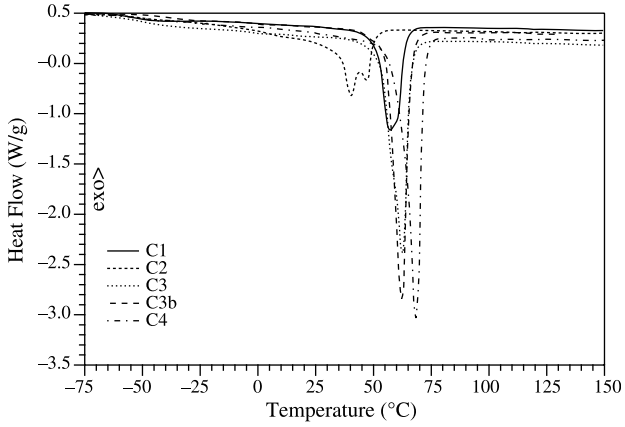

Fig. 3. DSC heating curves (10 °C/min) of C*x* copolymers.

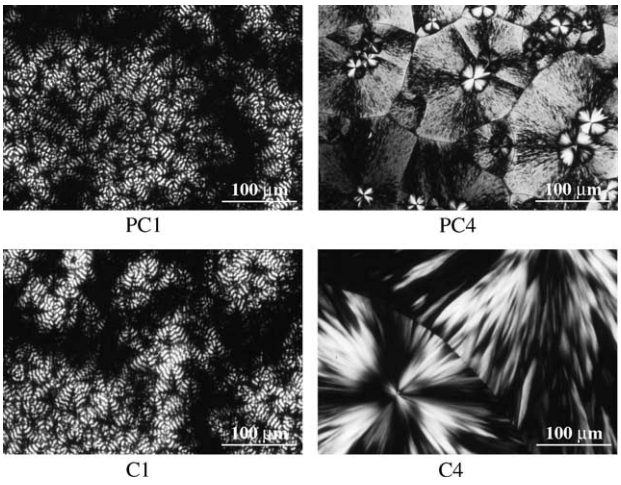

Fig. 4. Polarizing micrographs of representative PEG–PCL and PEG–PCL–PEG block copolymers crystallized at 25 °C.

copolymers equilibrated with Millipore water at 25 °C for 24 h. Samples were analyzed again after one week, and no significant variation was observed, suggesting that equilibration occurred within a few hours. On cooling from 30 to −50 °C, the sample thermograms displayed two exothermic transitions at about −10 and −25 °C attributable to the crystallization of free water and interfacial water, respectively. On heating from −50 to 30 °C, two endothermic transitions attributable to the melting of interfacial and free water were observed. The peak position of the former and the latter transitions moved from −17 to −2 °C and from 11 to 6 °C on increasing the PEG/PCL ratio (Table 5).

By taking into account the small water/polymer ratio, this trend seems to suggest that on increasing the polymer hydrophilicity, the interactions between interfacial water and the supposedly free water become more intense and the two peaks tend to merge.

The enthalpy of the endothermic peaks was used to compute the amount of interfacial water and free water, whereas bound water was evaluated as the complement to the total water content (Table 5). As expected, the interfacial water/polymer weight ratio increased from 0 to about 0.8 on increasing the molecular weight of MPEG from 350 to 5000. Correspondingly, the number of interfacial water molecules per oxyethylene unit (OE) increased from 0 to about 2.4. There is no obvious explanation for the absence of interfacial water in PC1 and C1 copolymers. One can tentatively propose that in the most hydrophobic samples, PEG chains are too short to form microcavities in which interfacial water can be trapped. As expected, PC*x* and C*x* copolymers derived from the same MPEG showed almost the same content of interfacial water. On the other hand, the bound water/polymer weight ratio increased from 0.30 to 0.48 (PC*x* samples) and from 0.13 to 0.32 (C*x* samples) on increasing the molecular weight of MPEG from 350 to 2000; a further increase of MPEG molecular weight to 5000 caused a decrease of this ratio to 0.29 (PC4) and 0.31 (C4). The number of bound water molecules per oxyethylene unit steadily decreased from 3.4 to 0.9 (PC*x* samples) and from 1.6 to 0.9 (C*x* samples) on increasing the PEG/PCL weight ratio. Apparently, the amount of bound water increased on increasing the polymer hydrophilicity and then decreased on increasing the copolymer water solubility. This behavior can be tentatively attributed to the increasing loosening of the polymer chains that causes the progressive relaxation of microcavities in which at least part of the bound water is trapped [41].

3.5. Critical micelle concentration

Amphiphilic PCL–PEG block copolymers should self-assemble in water. Accordingly, the occurrence of intermolecular association of the prepared polymers in water was investigated by fluorescence measurements, by using pyrene as fluorescence probe [42]. This technique is based on the different fluorescence spectrum of pyrene in water and included within the hydrophobic core of polymeric micelles (Fig. 5). Experiments were performed only on PC3, PC3b, PC4, and C2–C4 copolymers because of the poor water solubility of the other samples.

Table 5
State of water in the investigated polymeric materials

Sample	WPR	Free water		Interfacial water			Bound water	
		T_m (°C)	WPR	T_m (°C)	WPR	WOR	WPR	WOR
PC1	1.8	11	1.50	–	0	0	0.30	3.4
PC2	1.7	11	1.14	−12	0.05	0.3	0.41	2.5
PC3	1.8	9	0.88	−5	0.42	1.6	0.48	1.8
PC3b	1.8	9	0.85	−5	0.65	2.0	0.29	0.9
PC4	1.7	7	0.65	−2	0.80	2.4	0.29	0.9
C1	1.8	14	1.65	–	0	0	0.13	1.6
C2	1.8	9	1.42	−17	0.04	0.3	0.32	2.1
C3	1.8	9	1.05	−4	0.42	1.7	0.32	1.2
C3b	1.7	8	0.79	−4	0.64	2.0	0.31	1.0
C4	1.7	6	0.66	−4	0.73	2.2	0.31	0.9
PCL2000	1.7	12	1.70	–	0	0	0	0

WPR, water/polymer weight ratio; WOR, water/oxyethylene units molar ratio.

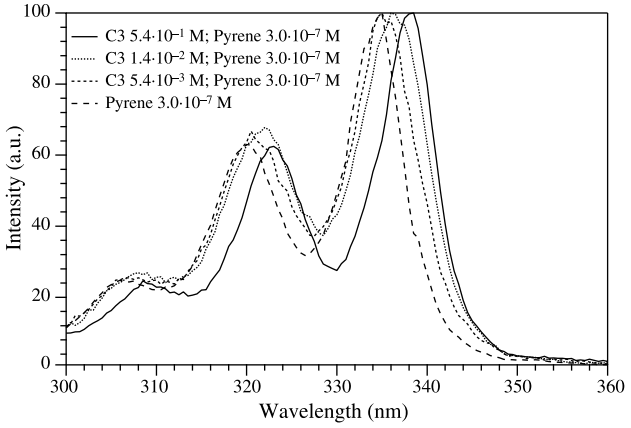

Fig. 5. Normalized excitation spectra ($\lambda_{ex}=390$ nm) of pyrene (3×10^{-7} M) recorded in the presence of increasing concentrations of C3 copolymer.

The intensity ratio of emission bands at 338 and 332.5 nm ($I_{338}/I_{332.5}$) of 3×10^{-7} M pyrene solutions containing 0.5–2×10–5 g/l copolymer was monitored (Fig. 6). As expected, micelles were not formed at low polymer concentration, and the $I_{338}/I_{332.5}$ ratio was almost constant, close to the characteristic value of pyrene in water. At high polymer concentration (larger than 0.1 g/l), all pyrene was included in the copolymer micelles and $I_{338}/I_{332.5}$ again reached an almost constant value (Fig. 6).

The shift of pyrene from water to the micelle core occurred at the onset of micelle formation [42]. Therefore, this value was properly taken as the copolymer critical micelle concentration (CMC) (Table 6). The hydrophilic–lipophilic balance (HLB), defined as twenty times the weight fraction of the hydrophilic portion [43], was used for comparing the polymer hydrophilicity. At constant length of the PCL segment, the calculated CMC of ABA copolymers increased from 3.1 to 4.4 mg/l on increasing the copolymer HLB from 7.5 to 16.0 (Samples C2, C3, and C4). Rather surprisingly, the increase of the molecular weight of the PEG block from 750 to 5000 did not affect much the

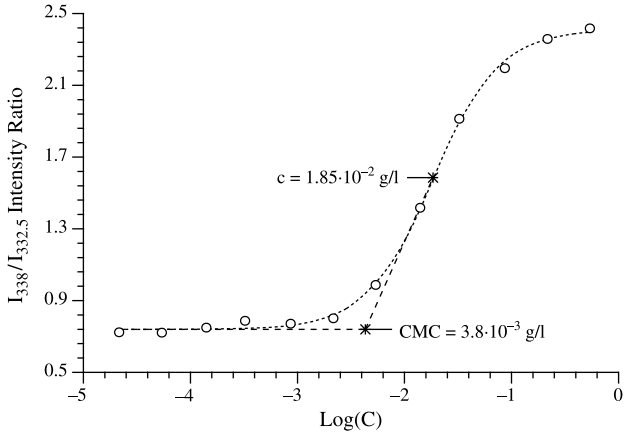

Fig. 6. Variation of $I_{338}/I_{332.5}$ fluorescence intensity ratio vs. C3 copolymer concentration.

Table 6
Hydrophilic–lipophilic balance (HLB) and critical micelle concentration of water-soluble block copolymers

Sample	MPEG M_n	PCL M_n[a]	HLB[b]	CMC (mg/l)[c]
PC3	2000	1150	12.7	9.9
PC3b	2000	500	16.0	158
PC4	5000	1150	16.3	7.1
C2	750	2300	7.5	3.1
C3	2000	2300	12.3	3.8
C3b	2000	1000	15.4	9.8
C4	5000	2300	16.0	4.4

[a] Determined by NMR measurements.
[b] Hydrophilic–lipophilic balance computed according to Ref. [31].
[c] Critical micellar concentration as evaluated by fluorescence measurements.

copolymer tendency to micellization. On the other hand, as expected [44], the CMC increased from 3.8 to 9.8 mg/l on decreasing the PCL block length from 20 (sample C3) to 9 (sample C3b). It is worth mentioning that the CMC of PC4 was appreciably higher than that of C4, although the two polymers have almost identical chemical composition and HLB. Comparison of C3b and PC3b samples shows an even larger CMC increase from 9.8 to 158 mg/l. The reported behavior clearly indicates that the ABA copolymer structure strongly favored micelle formation as compared to the AB enchainment. This effect can be tentatively attributed to the increased length of the PCL block in ABA copolymers as compared with the corresponding AB samples.

3.6. In vitro biological tests

In order to evaluate the biocompatibility of the prepared polymeric materials, in vitro experiments were carried out using 3T3/Balb clone A 31 mouse embryo fibroblast cell line [45].

3.6.1. Cell proliferation on polymer films

Cytotoxicity testing is a rapid, standardized, sensitive, and inexpensive way to assess the presence of significant amounts of biologically harmful extractable compounds in materials to be used in biomedical applications. Cell morphology and enzymatic activity are commonly used to investigate the material toxicity. The isolation of test cells in cultures and the absence of the protective mechanisms that assist the cells within the body guarantee for a high sensitivity [46]. The morphology of cells grown in presence of polymer films was similar to the one of cells grown on control materials (tissue culture polystyrene and glass) (Fig. 7). This indicates that the presence of polymer films did not interfere with the physiological assembling of cell cytoskeleton and with functions such as adhesion and spreading.

Quantitative evaluation of metabolically active cells after exposure to polymer films was performed by incubation of cells with tetrazolium salt WST-1. In viable

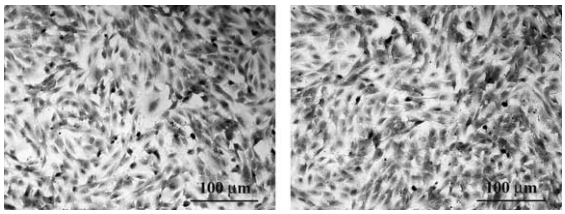

Fig. 7. Optical microscopy pictures of 3T3 cell cultures grown on glass (left) and on PC3 film (right) for 48 h.

cells, mithocondrial dehydrogenase enzimatically converts WST-1 to formazan. In all cases, the cell viability was higher than 70% with respect to the control material (Fig. 8). Accordingly, all the investigated materials can be defined as cytocompatible [47]. This result also indicates that the adopted purification procedure allowed for the removal of most $SnOct_2$, a compound known to be cytotoxic [48].

3.6.2. Cytotoxicity of soluble polymers

Some of the synthesized polymers displayed a suitable solubility in Dulbecco's Modified Eagles Medium (DMEM), thus allowing for the investigation of their IC_{50} (50% inhibitory concentration, that is the material concentration at which 50% of cell death in respect to the control is observed). Polymeric materials were dissolved in DMEM either at 10 mg/ml or at their maximum solubility. Cells were incubated for 24 h with the copolymer solutions and then analyzed for viability with WST-1 tetrazolium salt. In all cases, cell viability was close to 100% for all tested materials (Table 7). Therefore, the copolymer IC_{50} must be appreciably higher than 5–10 g/l, although it was not possible to evaluate its value, due to the limited solubility of the investigated materials in DMEM.

4. Conclusion

Amphiphilic diblock and triblock block copolymers consisting of alternating poly(ethylene glycol) (PEG) and poly(ε-caprolactone) (PCL) segments can be easily prepared in good yields by $SnOct_2$ catalyzed ring opening polymerization of ε-caprolactone initiated by monomethoxy-terminated poly(ethylene glycol) (MPEG). Coupling of two AB copolymer equivalents with 1 equiv of hexamethylene diisocyanate allows for the attainment of ABA (formally ABBA) block copolymers. The copolymer hydrophilic–lipophilic balance (HLB) can be tailored by suitable tuning of both MPEG and PCL degree of polymerization. Because of their blocky structure, these materials are characterized by a tendency to phase separation, both in bulk and in solution. In agreement, most of the prepared materials form micelles in water, as determined by fluorescence measurements using pyrene as fluorescent probe. As expected, the copolymer structure appreciably affects the critical micellar concentration (CMC). Indeed, the CMC progressively increases as PEG content increases; at comparable PEG chain length, the CMC strongly increases as PCL block decreases. The lack of in vitro toxicity, as indicated by cytocompatibility tests, as well as the tunable hydrophilic–lipophilic balance clearly supports the potential of the prepared polymeric materials in biomedical applications.

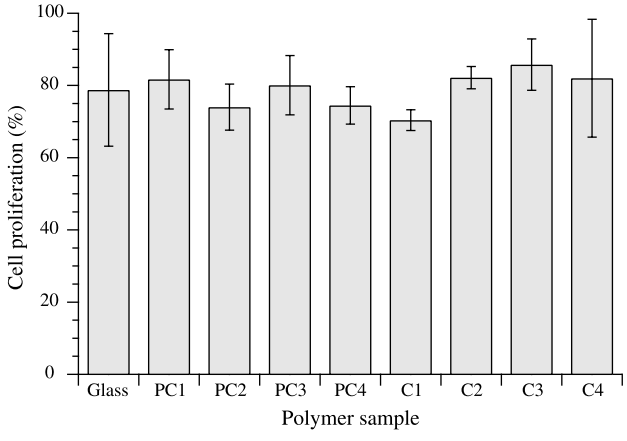

Fig. 8. In vitro toxicity of the investigated block copolymers.

Table 7
Evaluation of the cytotoxicity of water-soluble block copolymers

Sample	Concentration (mg/ml)	Cell proliferation (%)
PC3	6.0	100
PC3b	10.0	97
PC4	10.0	80
C3	5.8	100
C3b	10.0	100
C4	10.0	100

In DMEM at 37 °C.

Acknowledgements

The partial financial support by MIUR Prin project and EU funded TATLYS project is gratefully acknowledged. The authors wish to thank Miss Marcella Ferri who performed ABA copolymer fractionation and Dr. Tarita Biver for her help in recording fluorescence spectra.

References

[1] Zhang S. Nat Biotechnol 2003;21:1171–8.
[2] Roesler A, Vandermeulen GWM, Klok HA. Adv Drug Deliv Rev 2001;53:95–108.
[3] Cannizzaro SM, Padera RF, Langer R, Rogers RA, Black FE, Davies MC, et al. Biotechnol Bioeng 1998;58:529–35.
[4] Benhamed A, Ranger M, Leroux JC. Pharm Res 2001;18:232–328.
[5] Chung TS, Cho KY, Le HC, Nah JW, Yeo JH, Akaike T, et al. Polymer 2004;45:1592–7.
[6] Yang Z, Crothers M, Ricardo NMPS, Chaibundit C, Taboada P, Mosquera V, et al. Langmuir 2003;19:943–50.
[7] Oh KT, Bronich TK, Kabanov AV. J Controlled Release 2004;94:411–22.

[8] Lee J, Cho EC, Cho KY. J Controlled Release 2004;94:323–35.
[9] Jeong B, Bae YH, Wu KS. J Controlled Release 2000;63:155–63.
[10] Jeong B, Bae YH, Kim SW. Macromolecules 1999;32:7064–9.
[11] Shin IG, Kim SY, Lee YM, Cho CS, Sung YK. J Controlled Release 1998;51:1–11.
[12] Sosnik A, Cohn D. Polymer 2003;44:7033–42.
[13] Bogdanov B, Vidts A, van Den Bulke A, Verbeeck R, Schact E. Polymer 1998;39:1631–6.
[14] Piao L, Dai Z, Deng M, Chen X, Jing X. Polymer 2003;44:2025–31.
[15] Huang MH, Li S, Coudane J, Vert M. Macromol Chem Phys 2003; 204:1994–5.
[16] Choi YK, Bae YH, Kim SW. Macromolecules 1998;31:8766–74.
[17] Deng M, Chen X, Piao L, Zhang X, Dai Z, Jing X. J Polym Sci, Part A: Polym Chem 2004;42:950–9.
[18] Cammas-Marion S, Bear MM, Harada A, Guerin P, Kataoka K. Macromol Chem Phys 2000;201:355–64.
[19] Shuai X, Merdan T, Unger F, Wittmar M, Kissel T. Macromolecules 2003;36:5751–9.
[20] Yamamoto Y, Nagasaki Y, Kato Y, Sugiyama Y, Kataoka K. J Controlled Release 2001;77:27–38.
[21] Zhang S, Qing J, Xiong C, Peng Y. J Polym Sci, Part A: Polym Chem 2004;42:3527–36.
[22] Chiellini E, Solaro R, Leonardi G, Giannasi D, Lisciani R, Mazzanti G. J Controlled Release 1992;22:273–82.
[23] Solaro R, Dossi E, Chiellini E, Mazzanti G. J Bioact Comp Polym 1997;12:27–46.
[24] Chiellini E, Chiellini EE, Chiellini F, Solaro R. J Bioact Comp Polym 2001;16:441–65.
[25] Chiellini E, Covolan VL, Orsini LM, Solaro R. Macromol Symp 2003;197:345–54.
[26] Solaro R, Chiellini F, Signori F, Fiumi C, Bizzarri R, Chiellini E. J Mater Sci-Mater Med 2003;14:705–11.
[27] Bizzarri R, Chiellini F, Solaro R, Chiellini E, Cammas-Marion S, Guerin P. Macromolecules 2002;35:1215–23.
[28] Covolan VL, Di Ponzio R, Chiellini F, Grillo Fernandes E, Solaro R, Chiellini E. Macromol Symp 2004;218:273–82.
[29] Signori F, Solaro R, Chiellini E, Lips PAM, Dijkstra PJ, Feijen J. Macromol Symp 2003;197:289–302.
[30] Chiellini F, Bizzarri R, Ober CK, Schmaljiohann D, Yu T, Solaro R, et al. Macromol Rapid Commun 2001;22:1285.
[31] Chiellini F, Bizzarri R, Ober CK, Schmaljiohann D, Yu T, Saltzman WM, et al. Macromol Symp 2003;197:369–80.
[32] Tuominen J, Kylmä J, Kapanen A, Venelampi O, Itävaara M, Seppälä J. Biomacromol 2002;3:445–55.
[33] Wunderlich B. Macromolecular physics crystal nucleation growth annealing. vol. 2. New York: Academic Press; 1976. p. 218.
[34] Ma D, Luo X, Nishi T. Polymer 1997;38:1131.
[35] Ma D, Luo X, Zhang R, Nishi T. Polymer 1996;37:1575.
[36] Shiomi T, Imai K, Takenaka K, Takeshita H, Hayashi H, Tezikac Y. Polymer 2001;42:3233–9.
[37] John MS, Andrade JD. J Biomed Mater Res 1973;7:509–16.
[38] Ahmad MB, Huglin MB. Polym Int 1994;33:273–7.
[39] Nakamura K, Hatakeyma T, Hatakeyma T. Polymer 1983;24:871–6.
[40] Higuchi A, Komiyama J, Iijima T. Polym Bull 1984;11:203–8.
[41] Quinn FX, Kampff E, Smyth G, McBrierty VJ. Macromolecules 1988; 21:3191–8.
[42] Wilhelm M, Zhao CL, Wang Y, Xu R, Winnik MA, Mura JL, et al. Macromolecules 1991;24:1033–40.
[43] Becher P, Schick MJ. Surfactants science series. vol. 23. New York: Marcel Dekker; 1987. p. 435–91.
[44] Huibers PDT, Lobanov VS, Katritzky AR, Shah DO, Karelson M. Langmuir 1996;12:1462–70.
[45] Hermand MF. In: Braybrook JH, editor. Biocompatibility assessment of medical devices and materials. Chichester: Wiley; 1997. p. 120–3.
[46] ISO 10993 [EN 30993] Part 10995: Test for cytotoxicity—in vitro methods.
[47] Montanaro L. Biomaterials 2001;22:59–66.
[48] Tanzi MC, Verderio P, Lampugnani MG, Resnati M, Dejana E, Sturani EJ. Mater Sci-Mater Med 1994;5:393–6.